Final Report

Reflected GPS power for the detection of surface roughness *patterns* in coastal waters

by

George F. Oertel and Thomas R. Allen

Laboratory for Coastal Remote Sensing and Environmental Analysis
Old Dominion University
Norfolk, VA 23529

for

NASA Langley Research Center
Hampton, VA

January 2000

TABLE OF CONTENTS

1.0 INTRODUCTION

Coastal bays formed by the barrier islands of Delaware, Maryland and Virginia are parts of a coastal region known as a "Coastal Compartment". The coastal compartment between the Chesapeake and Delaware Bays is actually the mosaic of landscapes on the headland of the interfluve that separates these large drainage basins (Oertel and Kraft, 1994). The coastal compartments form a variety of different-shaped waterways landward of the coastline. Shape differences along the boundaries produce differences in exposure to wind and waves. Different shoreface topographies seaward of the coastline also influence surface roughness by changing wave-refraction patterns. Surface-water roughness (caused by waves) is controlled by a number of parameters, including fetch, shielding, exposure corridors, water-mass boundary conditions, wetland vegetation and water depth in coastal bays. In the coastal ocean, surface roughness patterns are controlled by shoreface shoaling and inlet refraction patterns in the coastal ocean. Knowledge of wave phenomena in the nearshore and backbarrier areas is needed to understand how wave climate influences important ecosystems in estuaries and bays.

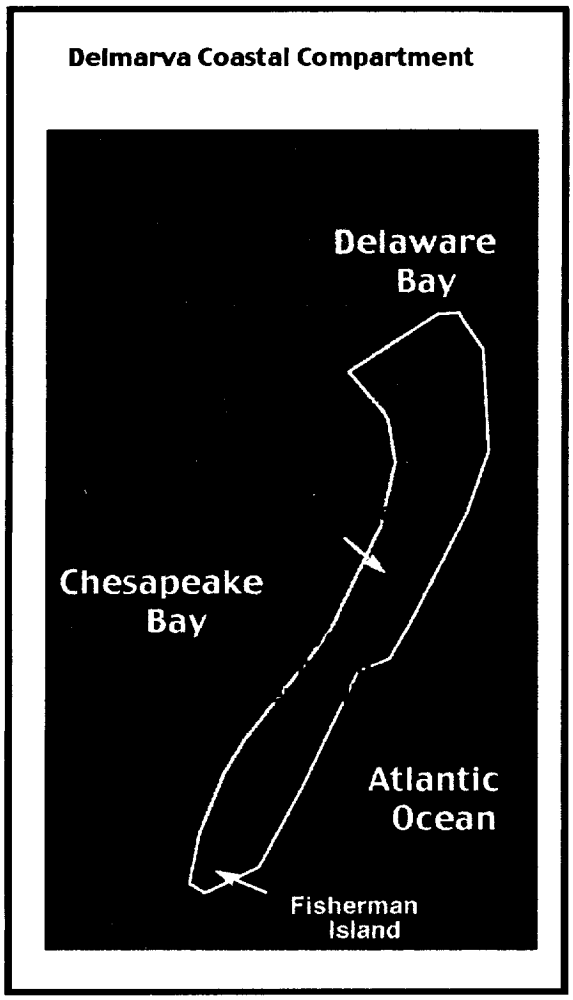

Figure 1 Nearshore environments of the Delmarva Coastal Compartment.

Research for this project was conducted by the Laboratory for Remote Sensing and Coastal Environmental Analysis (LaRCSEA) at Old Dominion University.

2.0 OBJECTIVES

The goal of this project was to evaluate the potential use of reflected global positioning system (RGPS) signals for identifying persistent areas of surface roughness in the coastal zone.

The NASA Langley Research Center (LaRC) is currently involved with flight tests of a new, remote sensing technology based on GPS power data. L-Band radiation of GPS signals reflects strongly from smooth flat surfaces such as water. Langley researchers have developed an airborne system which specifically detects reflected GPS (RGPS) signals (Katzberg and Garrison, 1996; Katzberg and Garrison, in press).

Initial tests indicate that vegetation and/or "rough" land surfaces do not reflect the GPS signal nearly as well as water, thus providing a tool for differentiation of the two surfaces. By utilizing the position information inherent in the GPS-based receiver, accurate location is easily derived. Unlike imaging satellite or other optical data, the GPS-based technique operates all-weather, day and night. It is relatively easy to integrate these data with existing digital maps and ground reference data. The GPS instrumentation consists of a modified GPS receiver and a specially modified GPS antenna looking downward. The current instrumentation is mounted on a B-200 KingAir owned by NASA-Langley Research Center and can be flown simultaneous to field verification. Data reduction software is available in addition to direct access to researchers' guidance in data interpretation. The NASA Wetlands Reflectance Group has already collected data from the coastal region and it is believed that "power scattering signal" may be related to surface roughness characteristics.

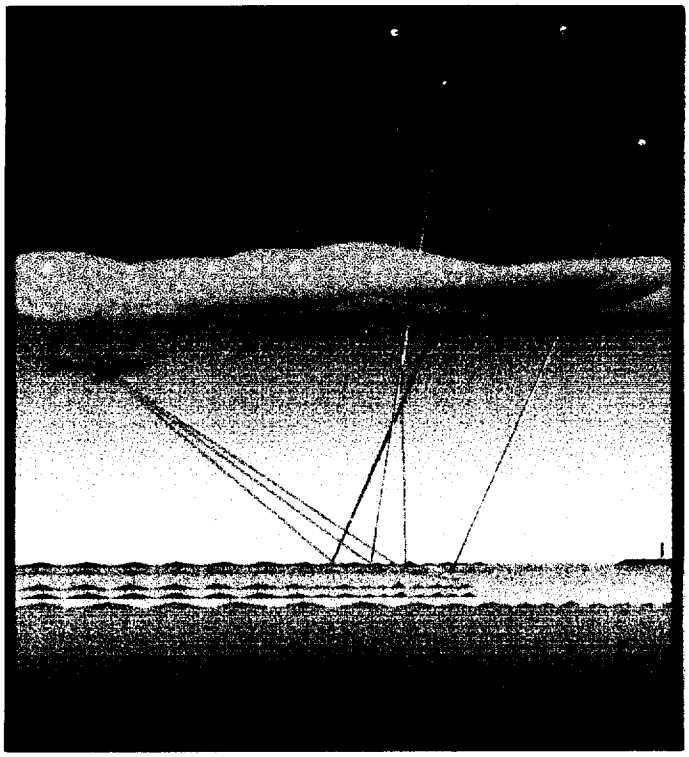

Figure 2 All-weather technique for evaluating water surface roughness characteristics.

The specific objectives are:

1) to use remote sensing imagery to identify where wetlands and specific surface-roughness characteristics are known to occur,

2) to determine if qualitative relationships exist between RGPS signal characteristics and surface roughness patterns,

3) to develop hypotheses for the qualitative analysis of surface characteristics and RGPS, where relationships are found.

3.0 RESULTS

3.1 Flight mission

On October 30 1998 a RGPS survey mission was flown over the coastal region of Fisherman Island using the NASA B200 Kingair aircraft. Both direct and reflected GPS data were collected from 6 satellites for about 1.4 hours (15:45:45 to 17:09:04 Eastern Time). During that time approximately 6,000 direct points of power were collected from an upward directed antenna, and

6,000 specular points were collected from a downward directed antenna. Using the differential time for direct and reflected signals and the azimuth and zenith of the satellites, the location of specular points were mapped on the Earth's surface. The flight path was designed to cross over the Chesapeake Bay, the coastal lagoon behind Fisherman Island, the marsh area on the backbarrier side of the island, the shallow shoreface in front of the island and the inlet area between Fisherman and Smith Island.

3.2 Flight Data

Flight transects started at the NASA Langley runway and proceeded over the Chesapeake Bay toward the Fisherman Island study area. Land cover along the flight line included open bay, ocean, nearshore and protected sounds of the Virginia barrier islands. Coastal terrestrial landscapes included beaches, vegetated dunes, interior cats-eye ponds, high marsh, and low marsh. The flight path also covered portions of open and shielded parts of the barrier lagoon and inlet.

3.3 Reformatting Raw Data

Basic steps in reformatting data included data file transfer from NASA Langley to LaRCSEA lab at Old Dominion University, relating multiple GPS attribute files together to link direct and reflected signal power values by common GPS timestamp, and mapping of specular reflectance points onto georeferenced images and GIS data layers.

Data were acquired from the NASA Langley Research Center (S.Katzberg) via anonymous FTP (file-transfer protocol.) These data included the raw receiver files, post-processed corrections, and ascii-coded records for specular point locations. Several steps had to be undertaken to integrate these datasets. First, the raw signals received direct from the satellite (top of plane antenna) needed to have the exact same timestamp (GPS time) so that these could be related to the specular points, subsequently processed and output in a separate file. Once integrated, these data also needed to be related to the individual satellite data, stored as power for each position, for each of six satellites. The result was a one-to-many relationship in the integrated file. Each second had six records, one for each of the incoming signals.

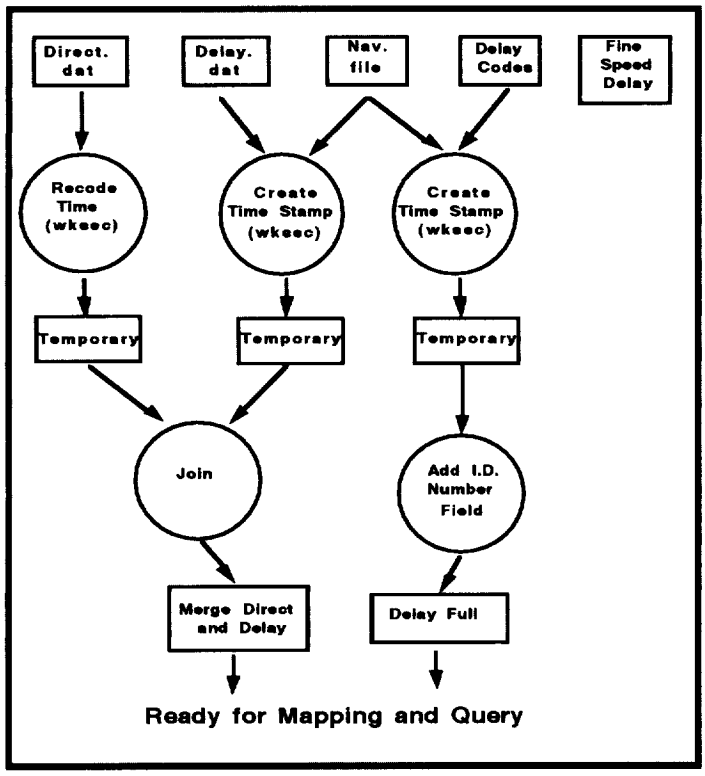

Figure 3 Flow chart illustrating data sources and merging techniques for analysis.

3.4 Data Integration

3.4.1 Digital Imagery and GIS Data

Several images and GIS data sources were integrated for statistical comparison, and visual display of RGPS data in map form. ArcView GIS (ESRI) was used as the primary platform for this integration and data storage. Imagery included Landsat-5 Thematic Mapper (TM) digital data (May 4, 1998), Spot PAN panchromatic image (July 20, 1994), land cover from a Landsat image classification (1993), AVIRIS hyperspectral airborne image (September 4, 1998), and color infra-red and black/white aerial photography (1997.) Ancillary GIS data included subset data for the Fisherman Island quadrangle: scanned USGS topographic quadrangles (1:24,000), U.S. Fish and Wildlife National Wetland Inventory (NWI) maps (1:24,000), USGS 1:24,000 Digital Elevation Models (DEMs) and Digital Line Graphs (DLGs.)

3.4.2. Oceanographic Data

Wave height data were acquired from the NOAA National Data Buoy Center website (http://seaboard.ndbc.noaa.gov/) for the October 30, 1998 flight. Detailed wave data were recorded for documenting the general wave conditions for two sites, the Chesapeake Bay Light Tower (CHLV-2) at 36.9N, 75.71W and the Virginia Beach Buoy (44014) at 64 nautical miles east of Virginia Beach (36.58N, 74.83W.) Buoy data for the overflight period are given in Table 1.

Parameter	CHLV2-Chesapeake Light	44014-Virginia Beach Buoy
Wind Direction, Speed	W (270 deg), 5.8 kts	(260 deg), 11.7 kts
Significant Wave Height	3.3 ft	4.3 ft
Wind-Wave Height	3.3 ft	4.3 ft
Wind-Wave Period	7.7 sec	7.7 sec
Wave Steepness	Average	Average
Average Wave Period	5.9 sec	5.8 sec

Table 1. Summary of buoy observations recorded at 1:00 p.m. EST, Oct. 30, 1998.

Winds during the overflight were weak and westerly. The wind field allowed little development of locally formed gravity waves. The water surface in the survey area was not "choppy" but had ripples related to the light winds. These phenomena were too small to be refracted by changes in nearshore bathymetry. The surface roughness phenomena were induced by the progression of waves that originated far from the survey area. Wave conditions were typical of "deep-water" waves related to offshore storms systems. The declining wave height conditions are consistent with the passage of a storm system (**Figure 3.**). In contrast to the locally formed ripples, these four-foot seas with 8s periods were large enough to be refracted by changes in nearshore bathymetry. Refraction

was expected to increase wave height and steepness in the nearshore zone and around the Smith Inlet shoals.

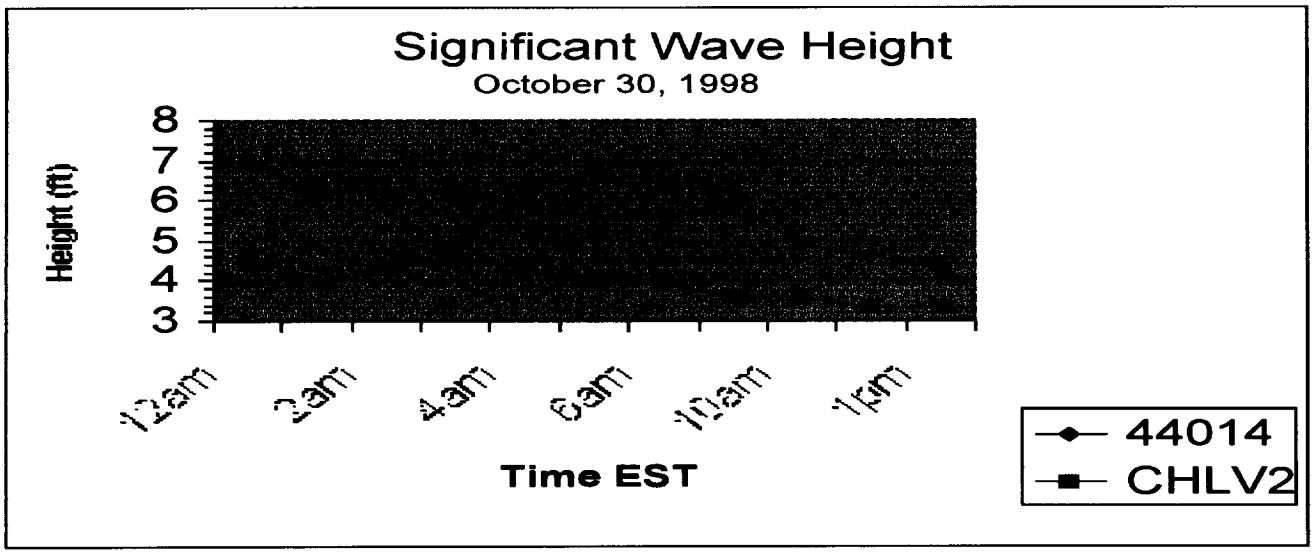

Figure 3 Significant wave heights over duration of October 30 flight from NOAA National Data Buoy Center for Virginia Beach Buoy (station 44014) and Chesapeake Light Tower (CHLV2.)

Tides also played a role in the roughness analysis of the survey area. The tidal phase effects the relative depth of the water in coastal areas, which affect the interaction of waves with the seabed. During high stages, offshore swell may pass over nearshore bars and inlet shoals. However, at low tide these bedforms cause waves to refract and change form. Land slopes around inland waters are often less than 0.5 degrees, and slight changes in tidal stage make cause significant exposures or inundations of land surfaces. At high tide, tidal flats and low-marsh wetlands are exposed, and although not covered by water the sediment moisture content of these surfaces remains high during periods of intertidal exposure.

Fisherman Island is located between the Wachapreague and Chesapeake Bay Bridge Tunnel Tides gauges. The tides at the Wachapreague Tide Station range from 3.25 feet at neap tide to about 6.25 at spring tide. The tides in the Chesapeake Bay entrance have a smaller range (between 2-4 ft). Wind stress and barometric pressure gradients may increase or decrease these ranges by 1-2 feet. The high tide at the Bay Bridge Tunnel station was measured at 3.5 feet on October 30, 1998.

During the October 30, 1998 RGPS survey (15:45 to 17:09 ET), the predicted high tide was for 16:00 ET and the marshes and tidal flat were inundated with water during the survey.

3.5 Partitioning the coastal setting into surface-roughness provinces

3.5.1 Island Provinces

Specular return from reflected GPS signals are controlled by static and dynamic phenomena. The static phenomena are an effect of the coastal landscape settings. At the microwave scale, the

weak presence of water may be detected by variations in the soil-moisture characteristics associated with different soils and plants. At Fisherman Island the vegetated and irregular, dry sandy surfaces are poorly reflective. Poorly reflective surfaces are primarily located in the upland areas of the island. Areas of greater specular return occurred on parts of the island that contained standing water (ponds) or in areas where soils contained high amounts of moisture. The ponds and wetland areas were readily delineated on 1997 Landsat TM image of Fisherman Island (fig. 4). High-moisture soils and high marsh wetlands were generally in narrow, low-elevation parts of the landscape. These areas were located based on the association with specific plant species. Four reflective subprovinces were designated for the island province (I):

Province	Subprovince	Description
I	a	Upland vegetated landscape
I	b	High-moisture soil and high-marsh wetlands
I	c	Low-marsh wetlands
I	d	Ponds

Table 2. Description of subprovinces on Fisherman Island Province

3.5.2 Water Provinces

Dynamic phenomena such as waves effect the roughness of the water surface. Two provinces were defined for water areas based on the characteristics of waves. Characteristics of waves effecting surface roughness were related to the [1] formation, [2] progression, [3] deformation and [4] dampening of waves. Coastal lagoons are shielded from offshore swell and have limited fetch, and shallow water depth. Flat water surfaces are highly reflective, whereas rough water surface tend to scatter microwaves before they can be reflected back to the GPS receiver. Four subprovinces were located in the coastal lagoon province.

Province	Subprovince	Description
II	a	Shielded coastal embayments (generally tranquil)
II	b	Limited-fetch areas (generally only capillary waves)
II	c	Wetted-areas with vegetative baffling
II	d	Open-fetch areas in coastal lagoons

Table 3. Description of subprovinces in Coastal Lagoon Province

The Chesapeake Bay and coastal ocean were treated as one province because of similarities in fetch, exposure and water depth. Six different subprovinces were discerned based on potential differences in local and deep-water wave generation and wave refraction (Table 4). The breaker

zone was discernible on the aerial photographs and satellite images. Wave crests were weakly discernible in these images.

Province	Subprovince	Description
III	a	Swash/wave-bore-breaker zone
III	b	Wave crest "bunching" and steepening,
III	c	Sea swell
III	d	Bay waves
III	e	Zone of wave-height enhancement at ebb tidal shoals
III	f	Deep ocean areas

Table 4. Description of subprovinces in Bay and Ocean

The 14 subprovinces that were located in the survey area were not all traversed by the overflight. Only 7 subprovinces were overflown and used for the analysis (see section 5.0 below).

4.0 NORMALIZING REFLECTED POWER

4.1 Raw Reflected GPS Power (RGPS) and Power Threshold Maps

Initially, RGPS data from early 1998 (pre-October 1998) surveys were draped over images of Fisherman Island to determine whether changes in the raw power return could distinguish different roughness signatures in the coastal environment. When draped onto 1m x 1m resolution photography, the RGPS signal could apparently discern most land/sea boundaries by a jump or drop in power (Figure 4).

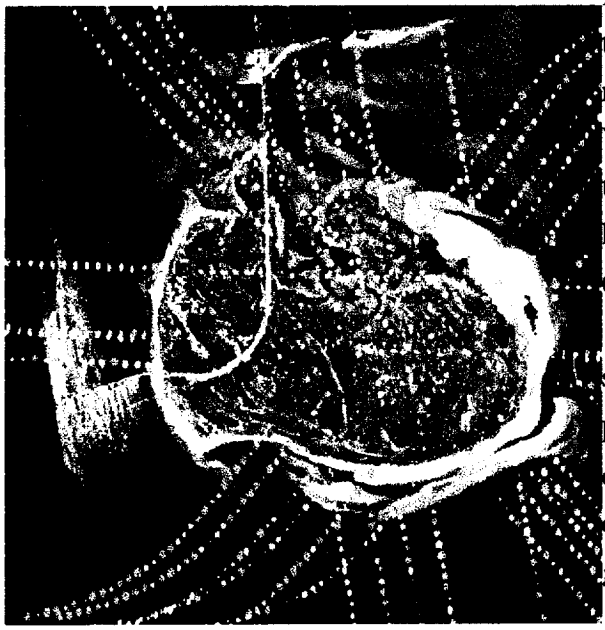

The yellow dots on figure 4 have three different sizes representing three arbitrary ranks of reflected power from different satellites. In general, larger dots occurred over the open-water areas and smaller dots occurred of the wetland areas, and dots were generally absent over the upland surfaces. Figure 4 is a B/W 1997 aerial photograph of Fisherman Island.

Figure 4 Threshold power evaluation in Spring 1998 (prior to October 30, 1998)

The width of the beach along the shoreline in 1997 changed slightly by 1998, and this may account for some of the boundary offset suggested by the ranked RGPS power. Also, the 1997 photo is a low-tide image and the early 1998 survey was conducted at high tide when the marshes and foreshore was inundated with water.

In October 30 1998 a RGPS survey mission was again flown over the Fisherman Island area, and reflected power was again simply ranked into three ordinal levels of power. Map plots of ranked GPS-reflectance power suggested the ability of RGPS to delineate the land-sea interface. However, qualitative or weak ordinal ranking of power values could not adequately discriminate effects of grazing angles with the surface or different wetland types (Figure 5). Figure 5 is a 1997 Landsat image of the southern tip of Smith Island. The dark dots are the GPS reference points of aircraft location.

The yellow dots are arbitrary ranks of reflected power from different satellites. When reflected power dropped below a minimum threshold, no dots were plotted. In this format, highly reflective surfaces were clearly discernable from poorly reflective surfaces. Water on the image is blue, vegetated dune ridges are red, low marsh is a dark brown-green and high marsh is a yellow-green. Note that dots are not present over the red (woody) areas on the image. This technique was insufficient to distinguish between high and low marsh areas.

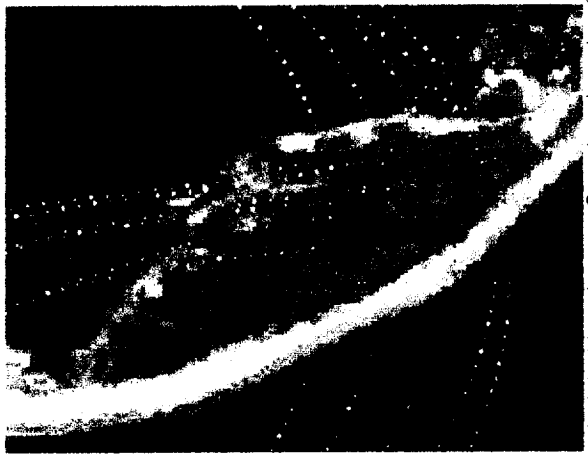

Figure 5 Close-up of ranked power threshold for Smith Island, VA.

In the raw data, no normalization of specular points was made using signal transmission strength or ionospheric delay. Specular points coinciding with land or water locations were distinct, although boundaries were indefinite.

Since variations in the raw power return showed some promise in distinguishing surface roughness variance, it was decided that a series of **algorithms should be developed to further calibrate and test the potential** mapping surface roughness characteristics.

4.2 Power Difference (PD)

The first attempt at calibrating the specular return signals for GPS satellites was to consider the power loss created by the surface roughness condition. Since the direct power from each satellite may vary, and the characteristics of the fresnel zone are related to the angle of the signal (satellite

altitude), then the direct minus the specular power is a first-order response to the effects of the scattering surface.

PD = Direct GPS Power - Specular GPS Power

The results of these manipulations appeared to have limited advantage over the raw threshold maps for distinguishing subtle differences in nearshore roughness phenomena (Fig. 6). The differences in PD values were illustrated as circles with different intensities of red. Dark red represented the highest PD value and light red represented low PD values. When draped over a 1997 aerial photograph of Fisherman Island. Variations in PD values were generally quite good for distinguishing land and water surface (although a few low values were present in known water locations). However, the variations in PD values over open water illustrated no evident pattern with respect to known differences in water surface roughness.

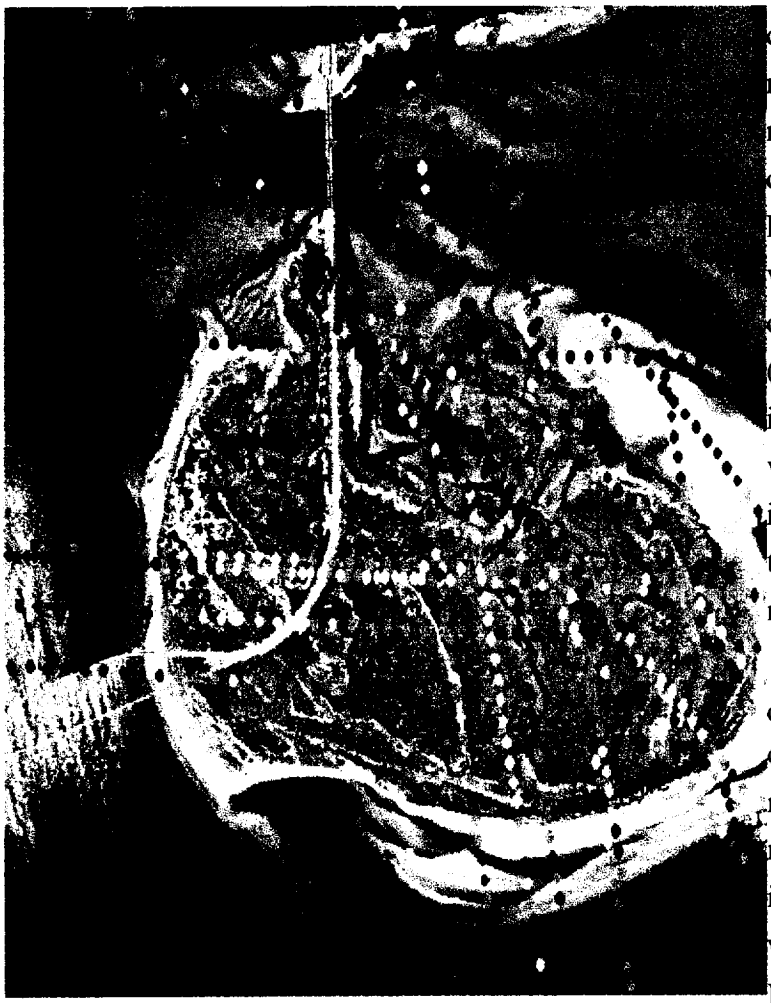

There appeared to be too much difference between the direct power outputs for the different satellites. This resulted in power variances that were more strongly influenced by differences in satellite power that differences that were created by characteristics of the Fresnel zone.

Figure 6 Relative direct-specular power difference applied to the whole Fisherman Island area.

4.3 Power Ratios (PR)

A second attempt to calibrate the specular return signals for GPS satellites was to normalize the power for each of the different satellites. A power ratio was calculated using the ratio of specular point power to direct power (recorded signal above the plane.)

PR = Direct Power / Specular Power

The normalized power ratio provides an alternative to simple difference, and provides an absolute real number allowing comparison of specular reflectance points. These data were also draped over the high-resolution 1997 aerial photography (Figure 7).

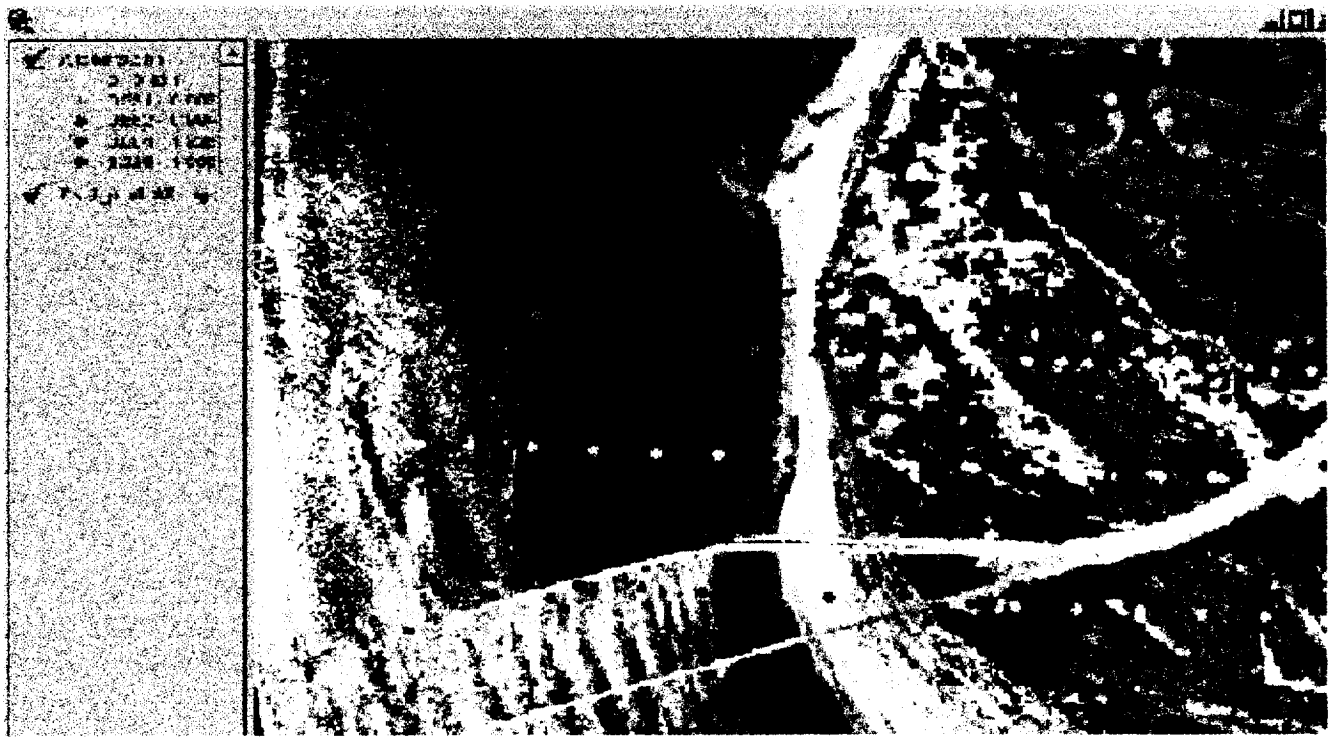

Figure 7 Ratio of direct:reflected GPS power for single swath and 6 SVs on west side of Fisherman Island. Points are draped onto a rectified 1997 B/W aerial photograph.

Figure 6 is an expanded section of the image that illustrates the shoreline along the southwest part of Fisherman Island and the Chesapeake Bay. The Sun glint on the image is a response to the 1997 surface conditions when the photograph was taken, and not when the 1998 RGPS mission was flown. The normalized power ratio data draped on the image illustrates RGPS specular return from 5 satellites. Again, the main ocean and island provinces have distinctly different values, but the boundary conditions were not precise for several satellites. Some of the boundary problems are related to the difference in tidal stage and the change in shoreline configuration between the 1997 photograph and the 1998 RGPS survey mission. The PR-specular return from the northernmost satellite (SR1) produced a good marker of the island and bay/ocean province. The PR-specular return from the southernmost satellite (SR5) was also good, since it is known that the shoreline retreated eastward between 1997 and 1998. There is no explanation for the high PR-specular returns over the island from the second satellite from the top. The third and fourth satellites produced returns that were immediately adjacent to each other. One set of returns produced an excellent gradient to establish the boundary between the island and bay/ocean province. The other set had consistently low PR-specular return over both the island and bay/ocean provinces.

As a result of the visual analysis of the ratios on the aerial photograph, it was still evident that the variation of direct power among satellites still effected a residual pattern. In some satellites, the signals apparently reflected strongly where others were weak. Further, the use of a ratio resulted in a wide scatter of values, making it difficult to compare the relative difference between direct and specular power peak. To further explore the processing of these values, a technique was used that involved power differences and a normalization to scale the difference (or ratio) to the range 0 - 1.0. This was called a normalized difference power ratio (NDPR).

4.4 Normalized Difference Power Ratio (NDPR)

The next step in attempting to relate RGPS data to surface scattering was made by normalizing the net power. The difference power (direct-specular) was normalized by dividing the difference by the sum (direct+specular):

$$\mathbf{NDPR = (Direct - Specular) / (Direct + Specular)}$$

This normalization scales the power difference within the range -1.0 to +1.0. The difference power (NDPR) plots over Fisherman Island were ranked by strength (Figure 8, values in Figure 8 were re-scaled by Arcview into 5 quantile classes) . The ranked data were illustrated on a 1997 aerial photo by color intensity of specular points. High NDPR values had more intense colors than low NDPR values which were represented by dots with faded colors. In general, the intense colors were located over the water areas, and the faded dots were located over the land and marsh areas.

Again, the 1997 aerial photo is a low tide image and the 1998 survey was conducted at high tide when the marshes and foreshore was inundated

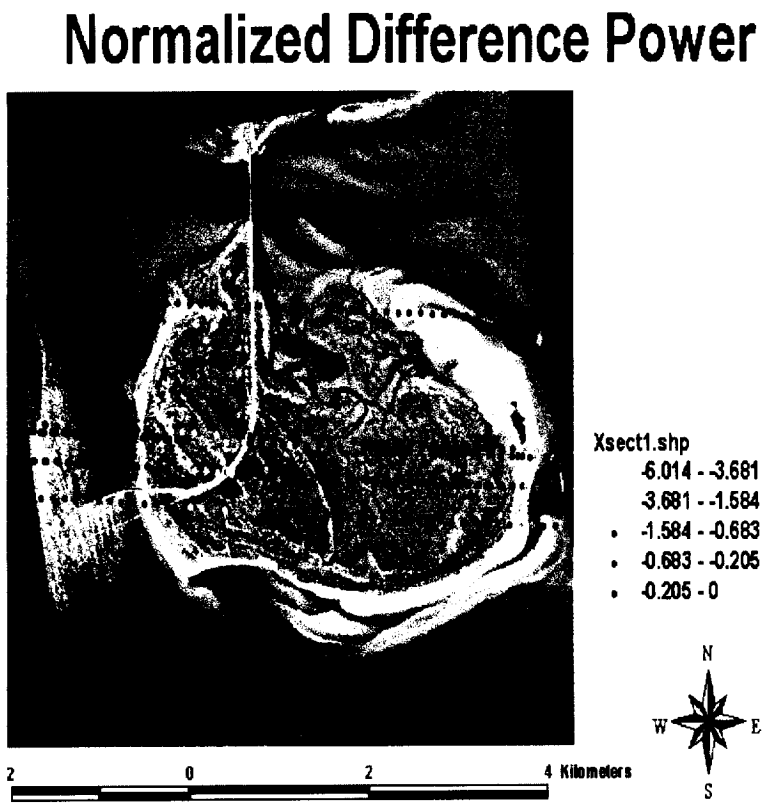

Figure 8 Quantile classes of normalized difference power (direct - specular) / (direct + specular).

with water. Some of the more intense colors that appear to be over sand bars, were probably submerged during the 1998 survey. This technique showed a considerable increase in differentiating power in areas of suspected wave refraction. Shielded bay and nearshore areas produced high NDPR values. Areas of known wave refraction around shoal and bars produced a mixture of NDPR values. On the graphic depiction (Fig. 8) they are illustrated by adjacent dots of clearly different hue intensity.

5.0 Mapping RGPS Signals and Coastal Provinces

The final component of the study was designed to assess the pattern of RGPS signals among seven different coastal settings: lagoons, marshes, upland, nearshore, ocean, bay and inlet. The method utilized manual digitization of the provinces onscreen. RGPS values were overlaid and extracted for each area (Fig. 9).

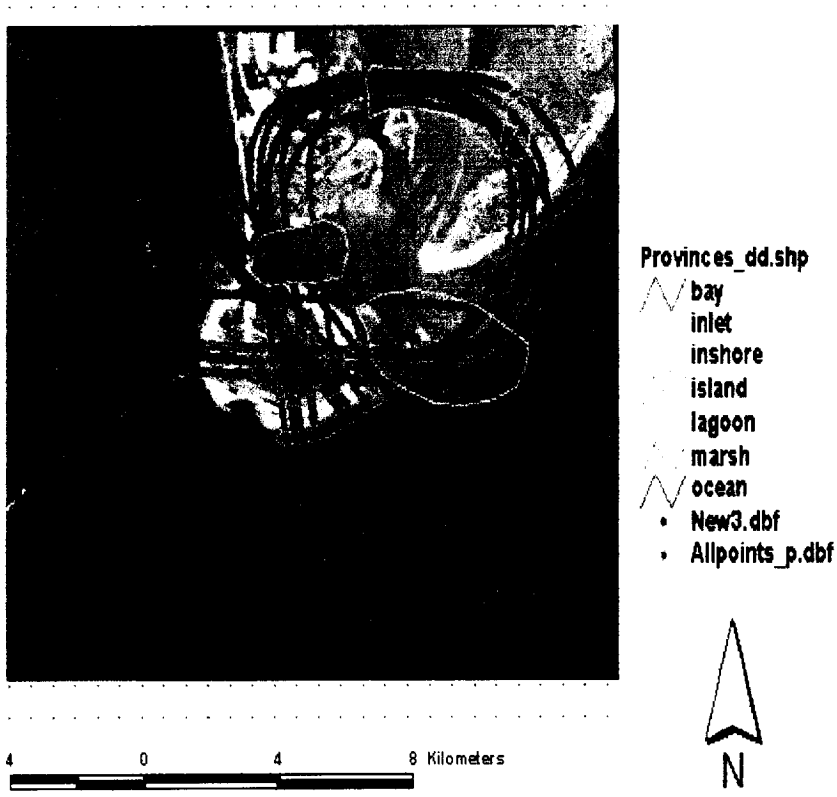

Statistical analyses included interpretation of summary descriptive statistics, box plots, and correlations among groups (Table 5 and Fig. 10). The use of discriminant classification analysis allowed us to assess whether groups were separable by their RGPS signals and to what degree.

Figure 9. Distribution of RGPS signals among coastal province sites of Fisherman Island.

Statistical results in Table 5 illustrate logical patterns differential GPS reflectance among coastal cover types. The mean power values (normalized by rescaling the ratio of direct signal to reflected signal for the range 0 - 1.0) for all water bodies are much stronger than those for upland and vegetated marshes. The lowest power is found in the mean for upland (0.337) while the highest average power is observed over inlet areas (0.58) followed by bay (0.543) and lagoon (0.542). The relative ordering among these marine environments reflects the conditions particular to this data acquisition, where conditions offshore in the Atlantic were choppy, with decreasing specular power for increasingly rough sea state. Interestingly, the nearshore wave environment, a zone affected by

steepening of wave facets and turbulence, was found to have a very low normalized GPS reflectance (0.388).

Province	N	Min.	Max.	Mean	Std. Dev.	Coeff. Var.
Lagoon	329	0.0001	0.997	0.542	0.281	0.518
Marsh	237	0.0000	0.984	0.387	0.243	0.627
Upland	192	0.026	0.988	0.337	0.238	0.706
Nearshore	63	0.007	0.985	0.388	0.291	0.749
Ocean	660	0.000	0.999	0.527	.0294	0.558
Bay	363	0.001	1.0	0.543	0.303	0.558
Inlet	183	0.007	1.0	0.580	0.296	0.510

Table 5. Summary statistics by coastal province for RGPS normalized power.

Figure 10 depicts box plots to further illustrate the pattern of RGPS signal strength, normalized by satellite direct power. The distributions were moderately wide for all provinces, however, the lower power cover types, marsh and upland had narrower ranges. This may reflect the relatively homogeneous diminution of signals in these vegetated surfaces. Nearshore areas had low reflectance but a larger range, possibly indicative of areas where wave heights vary across the

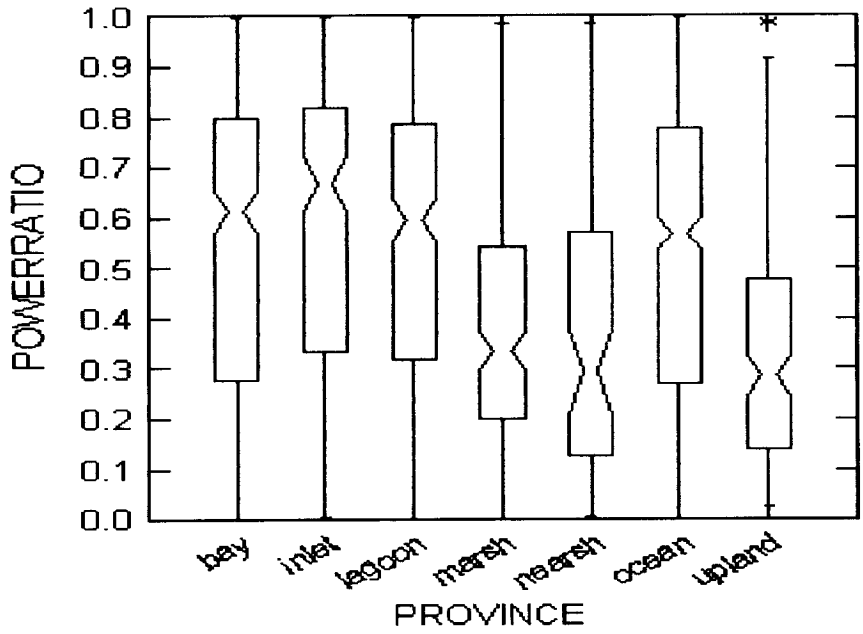

Figure 10. Box plots of RGPS power ratio by coastal province.

southern shore of Fisherman Island. There is a high degree of similarity among the distributions for bay, inlet, and lagoonal areas which all had relatively low wave energy conditions during the data acquisition. Ocean points were similarly wide in range but overall relatively lower in signal power.

The results above allow us to affirm our hypothesis, that RGPS signals differentiate areas of relatively high and low wave energy density (e.g., ocean/marine vs. enclosed bays and lagoons.) In addition, the convergence and steepening of wave crests evident in nearshore areas suggests that additionally, the RGPS signals convey patterns to wave energy density represented along a shoreline. The next component of the statistical analysis attempted to expand these results, to test whether the RGPS signals (normalized power) could be useful as a mapping technique by differentiating signal power characteristics.

We undertook a linear discriminant analysis of the coastal province RGPS data set. The objective was to apply a small set of RGPS power variables to determine 1) which power variable best differentiates actual surface features and 2) the degree of accuracy that surface features be classified using an RGPS signal. The discriminant analysis was done in Systat (vers. 8.0.) This technique produced a multiple variable ANOVA (F-matrix), created a set of canonical variates, and applied these independent variates to predict the type of surface (coastal province) using RGPS variables.

Among the possible predictor variables (RGPS specular power, ratio, difference, and normalized difference) the normalized power difference was found to provide the highest separability of the classes. While the classes would present multi-colinearity, the objective was to merely find the relative information content among these indices. The next step of the discriminant analysis provided new, uncorrelated canonical variates (factors) to predict province class from the RGPS power variables. The classification functions produced a matrix of classification accuracy. By percentages, the order of predictability from highest to lowest was: 1) upland (59%), 2) inlet (48%), bay (29%), lagoon (16%), nearshore (13%), marsh (8%), and ocean (6%). It is not surprising that upland areas (exhibiting low reflectance) would be the most predictable. The basic differentiation stands out among open water (ocean and bay), nearshore and inlet, and upland. Lagoonal, nearshore, and marsh areas were possibly affected by the time differential between the RGPS experiment (Oct. 1998) and the 1997 acquisition of the imagery and aerial photography used to interpret these locations. The time difference may have resulted in some of these areas actually changing cover characteristics, becoming inundated or dry. The overall accuracy of the discriminant classification, nonetheless, was 51%. This is a relatively weak classification, but offers insight into the basic assessment of coastal provinces which the RGPS data afford.

6.0 FUTURE DATA FORMAT REQUIREMENTS

Further research on RGPS mapping applications should seek to streamline the process of integrating the specular and direct data files within a geographic information system (GIS). This

will improve the ability to process more data (a larger number of flight missions and high-speed reflectance data, or interpolated points). In addition, it will save processing time for the GIS analyst to link and sort tables with few common fields. This integration would best be accomplished in the computer code that offloads or processes differential correction from the receivers. The optimal data formats would be similar to a RINEX file, preserving several of the original GPS time and satellite health variables. Two tables would be produced. The first would have a timestamp and include six records, with fields for direct and specular points. The second table would include the same timestamp or ID for each satellite with 32 columns for the power value at 32 values of the lag in time for each specular point. From these data, we could further explore the distribution of power through differentiation or integration. Subsequent statistics on these attributes may prove even more useful to mapping surface wave energy and coastal provinces.

7.0 CONCLUSIONS and SUGGESTIONS

Future experiments should seek to coincide data collection as closely as possible to available remote sensing platforms. We suggest the integration of SAR radar imagery, perhaps tasking the RADARSAT sensor, to assess the relationship between RGPS signals and wave height/energy. These could also be linked to Landsat Thematic Mapper or high resolution visible sensors to characterize coastal beaches and wave energy dissipation. Additional hazards applications could integrate the use of LIDAR data for characterizing dune, shoreface, and shoreline position relative to wave energy identified by RGPS, Radarsat, and fixed buoys. We would propose also conducting an experiment with satellite-based radar, RADARSAT, for characterization of sea surface roughness. Radarsat data could be acquired under the joint ADRO program of NASA ESE and the RADARSAT CANADA. Combined with LIDAR observations out at Wallops, both nearshore and offshore condtions could be related to RGPS data.

8.0 REFERENCES CITED

Katzberg, S. J. and Garrison, J.L. 1996. Utilizing GPS to determine Ionospheric delay over the ocean. NASA Tech. Memorandum 4750, NASA Langley Research Center, Hampton, VA

Katzberg and Garrison, in press. Surface reflected signals from the global positioning system for ionospheric measurements: experimental results at aircraft altitudes. Journ. of Atmospheric and Oceananic Technology,

Oertel, G.F. and J.C. Kraft, 1994. New Jersey and Delmarava Barrier Islands, In Davis (ed) Geology of barrier islands, Springer-Verlag, pp. 207-226.